

The Chemistry of Alkyl Iodides on Copper Surfaces. 1. Adsorption Geometry[†]

Cynthia J. Jenks[‡] and Brian E. Bent[§]

Department of Chemistry, Columbia University, New York, New York 10027

Neal Bernstein and Francisco Zaera^{*}

Department of Chemistry, University of California, Riverside, California 92521

Received: August 25, 1999; In Final Form: October 26, 1999

The adsorption geometries of iodomethane, iodoethane, 1-iodopropane, and 2-iodopropane on Cu(110) single-crystal surfaces were characterized by using reflection–absorption infrared spectroscopy. At 100 K adsorption is molecular in all cases, but with adsorption geometries that change with increasing coverages. All alkyl iodides adsorb with the C–I bond perpendicular to the surface at low coverages and tilted at saturation. The hydrocarbon chains in iodoethane, 1-iodopropane, and 2-iodopropane follow the expected behavior, namely, the first molecules chemisorb flat on the surface and those added above about half a monolayer adopt a vertical orientation. All the adsorbed alkyl iodides decompose by 140 K via the scission of their C–I bond and generate alkyl groups on the surface. Those surface alkyls also change configuration with coverage, aligning themselves at saturation in a fashion reminiscent of that seen in self-assembled monolayers.

1. Introduction

The chemistry of alkyl halides on copper surfaces is of relevance not only to industrial processes such as the Muller–Rochow direct production of organochlorosilanes^{1–3} and the Ullmann synthesis^{4,5} but also to the preparation of surface alkyl groups in model surface science studies.^{6–9} The utility of copper catalysts derives from their selectivity, since metallic copper can induce carbon–carbon coupling steps,^{10–14} sometimes exclusively without any side reactions.^{15–18} In addition, alkyl groups adsorbed on copper surfaces can also undergo β -hydride elimination to yield the corresponding olefin,^{19–23} a reaction typical of more reactive transition metals such as platinum^{24–26} and nickel.^{27–29} Finally, copper is quite efficient at breaking carbon–halide bonds (carbon–iodine bonds in particular),^{30,31} a property that is key in the production and disposal of halo hydrocarbons.³²

One of the main factors that controls the reactivity of adsorbed species on solid surfaces is their adsorption geometry. Two aspects of the geometry of adsorbates appear to be important for their chemistry. The first relates to the specific structure of the site where the adsorbate binds to the solid, the so-called ensemble effect that has been at the center of much of the discussion on hydrocarbon conversion selectivity.^{33–37} There is, however, a second more subtle and less discussed factor contributing to surface reactivity which has to do with the orientation of the molecular bonds of the adsorbates with respect to the surface plane. A good example of the latter effect is that of the activation of carbon monoxide on transition metals, which is known to be more likely on surfaces where the molecule bonds at an angle from the surface normal.^{38–40}

Adsorption geometries have in the past been obtained by diffraction techniques such as low-energy electron diffraction

(LEED)^{41–44} and X-ray photoelectron diffraction (XPD),^{45,46} or by taking advantage of the polarization dependence of electronic excitations in adsorbates, a property that is used in angle-resolved photoelectron spectroscopy (ARUPS)^{47–49} and near-edge X-ray absorption fine structure (NEXAFS).^{50–52} However, the data from those techniques are difficult to interpret, in particular when dealing with complex molecules.

Reflection–absorption infrared spectroscopy (RAIRS) has recently been incorporated into the group of surface characterization techniques for the study of adsorption geometries.^{53–56} One of the main advantages of infrared spectroscopy in surface studies is that it is quite sensitive to the details of the adsorbate studied: the vibrational modes identified by the interaction of IR radiation with matter are among the most molecule specific, and thus among the most informative for chemical identification. Not only vibrational frequencies are easily assigned to specific localized vibrational groups within a molecule (metal–adsorbate vibrations, O–H stretches, C–C–C deformation modes, etc.), but their values can also be used to speculate on the local environment in which the probed moiety is placed.^{57,58} More to the point of this report, additional geometrical information can be obtained by using the so-called surface selection rule, which states that on metals only vibrational modes with dynamic moments which have components perpendicular to the surface plane can be detected by RAIRS.⁵⁹ The relative intensities of the different vibrational modes of a given adsorbate can therefore be used to estimate the orientation of the corresponding moieties. This rule has been particularly useful in the study of self-assembled and Langmuir–Blodgett monolayers, where RAIRS data have been unique in providing information on the orientation of the hydrocarbon chains,⁶⁰ but it has also been used in surface science studies of small hydrocarbons under vacuum.^{61–65}

In this report, we present RAIRS data for a number of alkyl iodides adsorbed on Cu(110) single-crystal surfaces. Our results point to the specific adsorption geometry of the alkyl iodides themselves as well as that of the alkyl surface moieties produced

* To whom correspondence should be addressed.

[†] Part of the special issue "Gabor Somorjai Festschrift".

[‡] Present address: Ames Laboratory, Iowa State University, Ames, IA 50011.

[§] Deceased.

upon thermal activation of the C–I bond. A change in adsorption geometry is observed during the uptake of all the alkyl iodides at low (100 K) temperatures where the first C–C bond switches from flat-lying after low doses to standing up around monolayer saturation. However, in contrast to the case of iodoalkanes on Pt(111),⁶¹ there is no evidence for a collective rearrangement of the chemisorbed species on copper as the coverage is increased; only the new molecules appear to adsorb with the new upright orientation. Perpendicular metal–carbon bonding orientations are seen for the alkyl groups produced by thermal activation of adsorbed iodides above 180 K. The terminal methyl moieties in the corresponding alkyl iodides switch their orientation upon their conversion to alkyl surface groups because of the removal of the C–I bond. The accompanying paper addresses the role of surface structure on reactivity in those systems.⁶⁶

2. Experimental Section

The experiments reported here were performed in an ultrahigh vacuum (UHV) chamber pumped to a base pressure below 1×10^{-10} Torr and equipped with an ion sputtering gun, an UTI-100C mass spectrometer for temperature-programmed desorption (TPD), and a Mattson Sirius 100 FT-IR spectrometer for reflection–absorption infrared spectroscopy (RAIRS).^{62,64,67} RAIRS was performed by focusing the IR beam from the spectrometer through a sodium chloride window onto the sample at grazing incidence, passing the reflected beam through a second sodium chloride window and a polarizer, and refocusing it onto a mercury–cadmium–telluride (MCT) detector. Most of the spectra presented in this paper correspond to the average of 1000 scans taken with 4 cm^{-1} resolution, ratioed against similarly obtained spectra for the clean surface prior to dosing. The typical noise level in these data was on the order of $2\text{--}5 \times 10^{-5}$ absorbance units (au) in the $1400\text{--}2200 \text{ cm}^{-1}$ region and about $4\text{--}7 \times 10^{-5}$ au above 2800 cm^{-1} . Longer IR scanning times were avoided because of the slow drifts in the performance of the instrument which leads to miscalculations in the baseline (each 1000 scan set took about 5 min to acquire). However, spectra from separate individual experiments were in some instances averaged to improve the signal-to-noise ratio. All the RAIRS spectra were taken at sample temperatures below 120 K.

The copper single crystal was cut in the (110) orientation, polished to a mirror finish using standard procedures, and mounted on a sample holder capable of cooling to 100 K and of resistive heating to above 1000 K, as described before.²¹ The temperature was measured with a chromel–alumel thermocouple inserted into a hole on the side of the crystal. The sample was routinely cleaned by cycles of sputtering with Ar^+ ions, first at 850–920 K and then at room temperature, followed by annealing in vacuum at 950 K. Iodine was removed from the surface between experiments by flashing to 950 K. All the iodoalkanes were purchased from Aldrich (99+% purity) and were subjected to several freeze–pump–thaw cycles before introduction into the vacuum chamber. Their purity was checked periodically by mass spectrometry. Gas exposures were performed by backfilling of the vacuum chamber using leak valves, and are reported in langmuirs ($1 \text{ L} \equiv 10^{-6} \text{ Torr s}$), not corrected for differences in ion gauge sensitivities.

3. Results

Figure 1 displays RAIRS data obtained for the uptake of iodomethane on Cu(110) at 100 K. Two main features are seen at low coverages, at 2909 and 1230 cm^{-1} , which are easily assigned to the methyl symmetric C–H stretching and deforma-

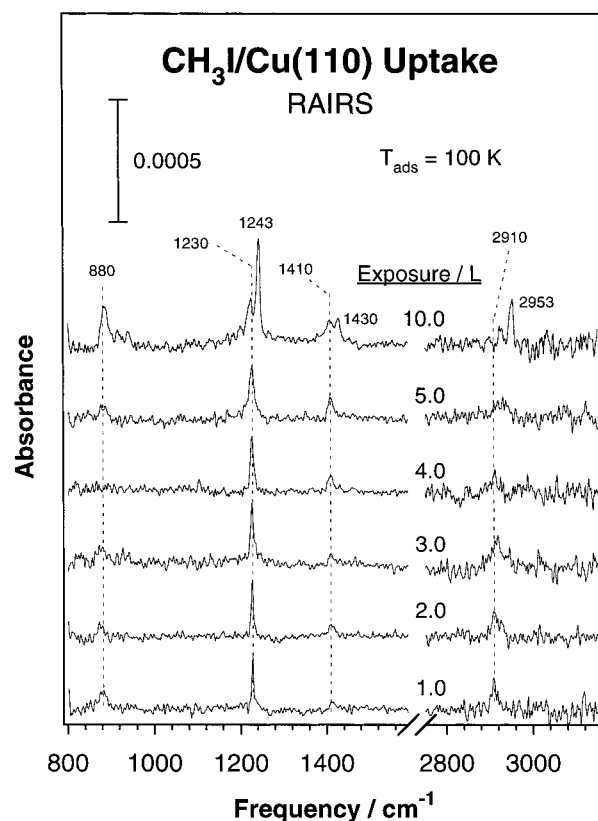


Figure 1. Reflection–absorption infrared spectra (RAIRS) for the uptake of iodomethane on a Cu(110) single-crystal surface at 100 K. Molecular adsorption is seen at this temperature, with an adsorption geometry that changes from a perpendicular configuration at low coverages to a more tilted orientation at saturation.

tion modes, respectively, by comparison with data from gas,^{68,69} liquid,⁷⁰ and solid⁷¹ iodomethane as well as with spectra from a $\text{CH}_3\text{I}/\text{Pt}(111)$ condensed film.⁷² Additional weaker signals are seen at about 1413 and 875 cm^{-1} corresponding to the methyl asymmetric deformation and rocking vibrations. The same peaks are seen all throughout the uptake of iodomethane until saturation of the first layer, which is reached after a dose of approximately 5.0 L CH_3I , except that the relative intensities of the different peaks change with increasing exposure, the asymmetric deformation feature growing at the expense of the symmetric deformation signal. The spectrum for the 10.0 L exposure shows the band splitting due to crystal fields in the solid,⁷¹ indicating the start of the build up of a multilayer. The peak assignments for this system as a function of exposure are provided in Table 1 together with the appropriate reference data.

Figure 2 shows the RAIRS traces for the uptake of iodoethane on Cu(110) at 100 K. The assignment of the vibrational modes in this case can also be easily done by comparison of the spectrum of an iodoethane multilayer condensed at 100 K (30.0 L exposure, top trace in Figure 2) with those reported in the literature for liquid and solid iodoethane.^{73,74} By and large, the features seen in the iodoethane/copper system are those of the terminal methyl group; the symmetric deformation (umbrella) mode at 1377 cm^{-1} , the asymmetric deformations at 1433, 1440, and 1447 cm^{-1} , and the symmetric and asymmetric C–H stretchings at 2916 and 2970 cm^{-1} , respectively, match nicely those seen in the solid phase. Three other features are also evident in our spectra, namely, a C–C stretching mode at 951 cm^{-1} , a CH_2 twist around 1204 cm^{-1} , and the methyl asymmetric deformation first overtone at 2860 cm^{-1} . A summary of these assignments is provided in Table 2.

TABLE 1: Vibrational Assignments (in cm^{-1}) for the Infrared Spectra of Iodomethane Adsorbed on Cu(110) at 100 K as a Function of Exposure, with the Assignments for Both an Iodomethane Layer Condensed on Pt(111) and Liquid Iodomethane Provided for Reference

normal mode ^a	CH ₃ I/Cu(110), 100 K ^{b,c}			2.0 L CH ₃ I on Pt(111) ^{b,d}	liquid CH ₃ I ^{b,e}
	2.0 L	5.0 L	10.0 L		
$\nu_a(\text{CH}_3)$		2945 w	2953 m		3067
$\nu_s(\text{CH}_3)$	2909 m	2925 w	2922 w	2920 m	2950
$\delta_a(\text{CH}_3)$	1413 w	1409 m	1409 m	1409 m	1424
			1430 m		
$\delta_s(\text{CH}_3)$	1230 s	1227 s	1227 m	1225 s	1235
			1243 s		
$\rho(\text{CH}_3)$	875 m	880 w	883 m	874 m	880

^a Notation: s and a = symmetric (A_1) and asymmetric (E) with respect to the three-fold symmetry axis of the CH₃ group, respectively.

^b Notation: s = strong, m = medium, and w = weak. ^c This work.

^d From ref 72. ^e From ref 70.

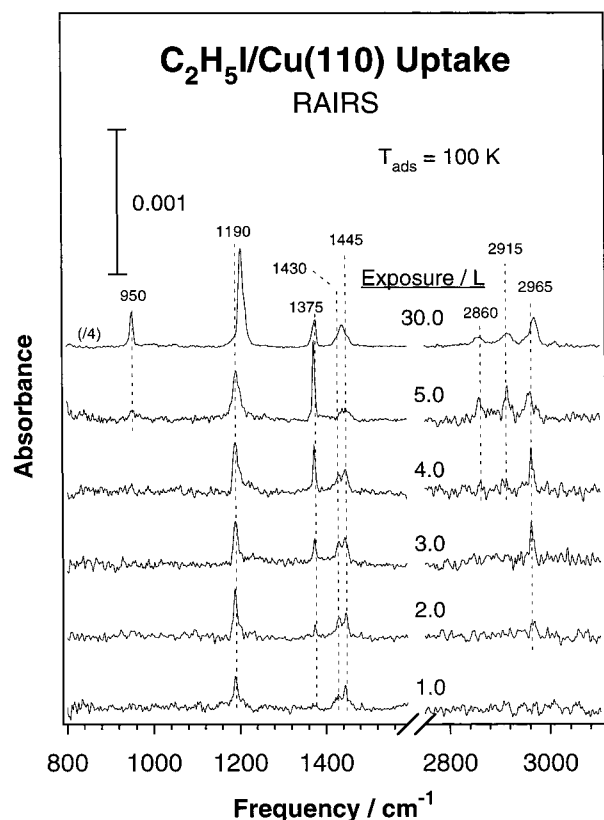


Figure 2. RAIRS data for the uptake of iodoethane on Cu(110) at 100 K. The C—C bond orientation in the adsorbed iodide in this case changes from parallel to the surface at low coverages to vertical at saturation, but only the additional molecules above half a monolayer adopt the new configuration.

It can also be seen from Figure 2 that the peak frequencies for the case of low iodoethane exposures are virtually the same as those in the multilayer RAIRS spectrum, but that their relative intensities are substantially different. For instance, the C—C stretching peak at 951 cm^{-1} , having a significant intensity in the multilayer, is virtually invisible in the submonolayer spectra. Furthermore, the relative peak heights in the submonolayer spectra change drastically with coverage. Note in particular the development of the methyl symmetric and asymmetric deformation peaks [$\delta_s'(\text{CH}_3)$ and $\delta_a'(\text{CH}_3)$] at 1377 and 1444 cm^{-1} , respectively, with increasing dose: after a 1.0 L exposure the $\delta_s'(\text{CH}_3)$ mode can barely be detected, but by 5.0 L that peak dominates the spectrum. A complete assignment of the peaks as a function of exposure is provided in Table 2, and the

TABLE 2: Vibrational Assignments (in cm^{-1}) for the Infrared Spectra of Iodoethane Adsorbed on Cu(110) at 100 K as a Function of Exposure, with Assignments for Both an Iodoethane Film Condensed on Pt(111) and Solid Iodoethane Provided for Reference

normal mode ^a	C ₂ H ₅ I/Cu(110), 100 K ^{b,c}				5.0 L C ₂ H ₅ I on Pt(111) ^{b,d}	solid C ₂ H ₅ I ^{b,e}
	1.0 L	3.0 L	5.0 L	30.0 L		
$\nu_a'(\text{CH}_3)$		2963 s	2960 m	2970 s	2952 w	2968 s
$\nu_s'(\text{CH}_3)$			2915 m	2916 m	2914 m	2908 m
$2\delta_a''(\text{CH}_3)$			2860 w	2860 w	2857 m	2848 m
$\delta_a'(\text{CH}_3)$	1444 s	1444 m	1447 w	1440 m	1445 br	1452 m
				1447 sh		
$\gamma'(\text{CH}_2)$	1429 m	1429 m	1440 w	1433 w		1419 m
$\delta_s'(\text{CH}_3)$	1373 w	1374 m	1375 vs	1377 m	1370 s	1370 s
$\tau''(\text{CH}_2)$	1187 s	1189 s	1192 s	1204 s	1185 m	1199 vs
$\nu'(\text{C}-\text{C})$			951 w	951 m		949 s

^a Notation: prime (') = A' symmetry (C_s point group), double prime (") = A'' symmetry (C_s point group); s and a = symmetric and asymmetric (respectively) with respect to the three-fold symmetry axis of the CH₃ group or the two-fold symmetry axis of the CH₂ group.

^b Notation: vs = very strong, s = strong, m = medium, w = weak, sh = shoulder, and br = broad. ^c This work. ^d From ref 62. ^e From ref 73.

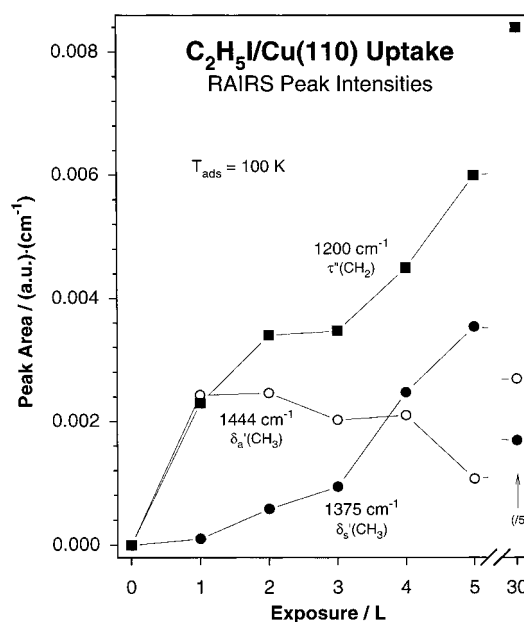


Figure 3. RAIRS peak areas for the uptake of iodoethane on Cu(110) at 100 K, as calculated from the data in Figure 2. Results are plotted for the symmetric [$\delta_s'(\text{CH}_3)$] and asymmetric [$\delta_a'(\text{CH}_3)$] methyl deformation modes at 1375 and 1444 cm^{-1} , respectively, as well as for the methylene twist [$\tau''(\text{CH}_2)$] at 1200 cm^{-1} . The rapid increase of the 1444 cm^{-1} peak intensity attests to the flat geometry of the terminal methyl moieties in the initial adsorbates, while the growth of the 1375 cm^{-1} feature above 3.0 L indicates the vertical configuration of the new molecules after that point.

variations of peak intensities with coverage for the modes corresponding to the methylene twist [$\tau''(\text{CH}_2)$, around 1200 cm^{-1}] and to the methyl symmetric and asymmetric deformations [$\delta_s'(\text{CH}_3)$, 1375 cm^{-1} , and $\delta_a'(\text{CH}_3)$, 1444 cm^{-1} , respectively] are displayed in Figure 3.

The assignments discussed above were corroborated by additional RAIRS data from partially deuterated iodoethanes. Figure 4 displays the vibrational spectra obtained after exposing the Cu(110) surface to 2.0 L of CH₃CH₂I (bottom), CH₃CD₂I (middle), and CD₃CH₂I (top) at 100 K. It can be seen there how the asymmetric stretching mode of the methyl group shifts from about 2965 cm^{-1} in CH₃CH₂I and CH₃CD₂I to 2225 cm^{-1} in CD₃CH₂I. Equally clear is the disappearance of the methyl

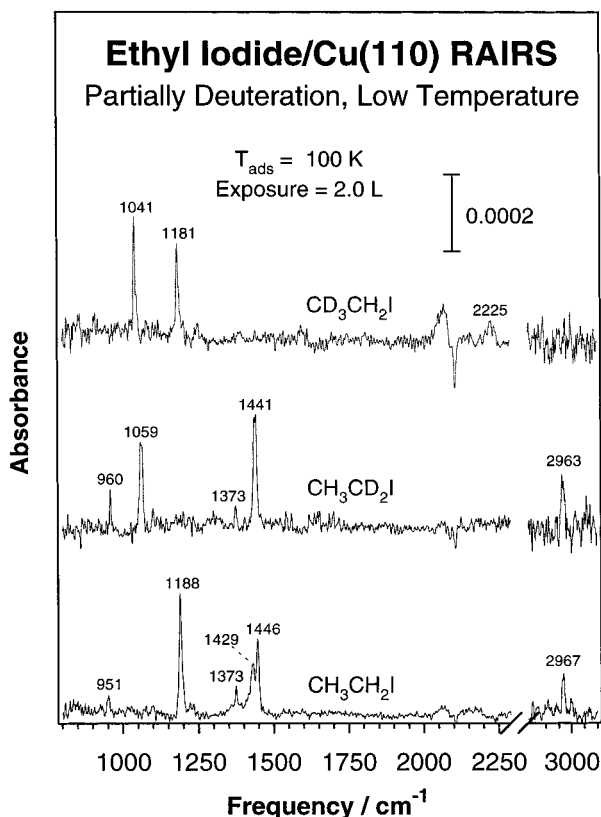


Figure 4. RAIRS data for 2.0 L of $\text{CH}_3\text{CH}_2\text{I}$ (bottom), $\text{CH}_3\text{CD}_2\text{I}$ (middle), and $\text{CD}_3\text{CH}_2\text{I}$ (top) adsorbed on Cu(110) at 100 K. These spectra were used to help in the identification of the methyl and methylene vibrational normal modes of molecular iodoethane.

symmetric deformation mode at approximately 1441–1446 cm^{-1} upon deuteration of that moiety. Less obvious are the changes in the vibrational bands associated with the methylene groups, except perhaps for the twist motion, which is only seen for $\text{CH}_3\text{CH}_2\text{I}$ and $\text{CD}_3\text{CH}_2\text{I}$ around 1181–1188 cm^{-1} . The C–C stretching peak is quite weak in all cases, but can be identified by its approximately constant value for the three compounds about 900–960 cm^{-1} . Table 3 provides the complete assignment of the peaks in these spectra.⁷³

RAIRS data from the initial product that forms after thermal activation of iodoethane on Cu(110) are provided in Figure 5. The lower trace, which corresponds to 2.0 L of $\text{CH}_3\text{CH}_2\text{I}$ dosed at 100 K, is consistent with the uptake data shown in Figures 2 and 4. Six main modes are observed in this case, at 2967, 1446, 1429, 1373, 1188, and 951 cm^{-1} , attributable to the $\nu_a'(\text{CH}_3)$, $\delta_a'(\text{CH}_3)$, $\gamma'(\text{CH}_2)$, $\delta_s'(\text{CH}_3)$, $\tau''(\text{CH}_2)$, and $\nu(\text{C}-\text{C})$ modes, respectively (see Tables 2 and 3). Annealing that surface at either 110 or 120 K for 30 s leads to the development of new bands at 2910, 2875, and 2840 cm^{-1} . The modes previously centered at 1445 and 1187 cm^{-1} also shift to 1443 and 1191 cm^{-1} , respectively, decrease in intensity, and change in relative size (the absorbance ratio varying from 0.7 to 0.5). A clear transition takes place on the surface around 140 K, at which point the IR spectrum displays almost no features in the deformation region, and a new species appears by 190 K. There are significant changes in the 1130–1450 cm^{-1} region between the spectra obtained for the 2.0 L iodoethane dose at 120 K and at 190 K: the methyl deformation peaks about 1373 and 1443 cm^{-1} almost disappear upon heating of the surface (the first shifts to 1363 cm^{-1}), and the methylene twisting mode shifts down to 1129 cm^{-1} . Also, there is a slight blue shift in the symmetric C–H stretching frequency from 2910 to 2914 cm^{-1} . Finally, annealing

to 250 K leads to the disappearance of most of the features in the infrared spectrum.

The identification of the new species that forms on Cu(110) upon heating adsorbed iodoethane to 190 K is aided by the RAIRS data of the partially isotopically labeled compounds shown in Figure 6. The bottom trace of that figure is a repeat of the one in Figure 5, and is included here solely for comparison purposes. The other two traces in this figure are the RAIRS results obtained after adsorption of 2.0 L of iodoethane-1,1- d_2 (middle) and of iodoethane-2,2,2- d_3 (top) on Cu(110) at 190 K. Given that the C–H stretching mode at 2914 cm^{-1} does not disappear upon deuteration of the surface ethyl group at the α position, it is assigned to the symmetric deformation of the terminal methyl moiety; that peak shifts to 2085 cm^{-1} in the β -substituted compound. Also, the modes at 1441 [$\delta_a'(\text{CH}_3)$] and 1363 cm^{-1} [$\delta_s'(\text{CH}_3)$] in the normal (fully hydrogenated) ethyl species do not shift by more than 2 cm^{-1} when replacing the α -hydrogens for deuteriums, but move down to 1121 and 1087 cm^{-1} (respectively) when the methyl group is deuterated. From all this it is clear that the methyl groups of the adsorbed iodoethane remain intact upon heating the sample to 190 K. The faith of the methylene moiety is harder to determine from these spectra, since no peaks clearly attributable to $\nu(\text{CH}_2)$ modes are observed for the β -deuterated iodoethane (most likely because of the low absorption cross section of those vibrations). The weak feature at 2874 cm^{-1} in the normal ethyl spectrum shifts to 2075 cm^{-1} upon α -deuteration, and is therefore most likely associated with the CX_2 groups; the significant red-shift of that mode when compared with molecular iodoethane is indicative of the strong interaction of the methylene end with the surface once the C–I bond is broken. The observed modes in Figure 6 and their assignments are tabulated and compared to the solid iodoethane infrared values in Table 3. On the basis of our data as well as of knowledge from previous systems, we interpret the data for the 190 K species as to correspond to ethyl surface groups.

The changes in adsorption geometry of the ethyl groups on Cu(110) were characterized further via the acquisition of RAIRS data for iodoethane on Cu(110) at 190 K as a function of exposure. Figure 7 displays the spectra obtained for the ethyl moieties prepared with 1.0, 2.0, 3.0, and 5.0 L doses. Again, the main characterizing features of this species at low coverages are the methyl symmetric stretch [$\nu_s'(\text{CH}_3)$] at 2914 cm^{-1} and the methylene twist [$\tau''(\text{CH}_2)$] around 1130 cm^{-1} . Additional bands are seen in the high coverage spectra at 2962 [$\nu_a'(\text{CH}_3)$], 2874 [$\nu_s'(\text{CH}_2)$], and 2840–2850 [$2\delta_a''(\text{CH}_3)$] cm^{-1} , together with weaker features for the methyl symmetric and asymmetric deformations [$\delta_s'(\text{CH}_3)$ and $\delta_a'(\text{CH}_3)$, at 1365 and 1450 cm^{-1} , respectively]. Finally, it is tempting to assign the peak around 1250 cm^{-1} to the methylene scissoring mode [$\gamma'(\text{CH}_2)$], even though that would imply a significant shift to the red from the energy of the corresponding vibration in the free molecule. Our assignment of the peaks in Figure 7 is provided in Table 3. The key information derived from Figure 7 is that the relative intensities of the main spectral features change with coverage. The inset displays data for two specific cases, the ratios of the symmetric to asymmetric C–H stretching modes [$\nu_s'(\text{CH}_3)/\nu_a'(\text{CH}_3)$, at 2914 and 2962 cm^{-1} , respectively] and of the symmetric C–H stretch to the twist of the methylene moiety [$\nu_s'(\text{CH}_2)/\tau''(\text{CH}_2)$, at 2874 and 1130 cm^{-1} , respectively]. These changes, which represent changes in adsorption geometry with coverage, are explained in the Discussion section.

Finally, a comparative study was carried out on the alkyl groups produced by different alkyl iodides over the Cu(110)

TABLE 3: Vibrational Assignments (in cm^{-1}) for the Infrared Spectra for 2.0 L of Iodoethane- d_0 , Iodoethane-1,1- d_2 , and Iodoethane-2,2,2- d_3 Adsorbed on Cu(110) at 100 K (molecular) and at 190 K (after the formation of ethyl groups on the surface), with the Assignments for the Corresponding Solid Iodoethanes Provided for Reference

mode ^a	Normal Iodoethane- d_0			Iodoethane-1,1- d_2			Iodoethane-2,2,2- d_3		
	on Cu(110) 100 K ^{b,c}	on Cu(110) 190 K ^{b,c}	solid ^{b,d}	on Cu(110) 100 K ^{b,c}	on Cu(110) 190 K ^{b,c}	Solid ^{b,d}	on Cu(110) 100 K ^{b,c}	on Cu(110) 190 K ^{b,c}	Solid ^{b,d}
$\nu_a'(\text{CX}_3)$	2967 m	2962 w	2968 s	2963 m		2955 m	2225 w	2193 s	2214 m
$\nu_s'(\text{CX}_3)$		2914 vs	2908 m		2914 vs	2910 m		2085 w	2111 w
$\nu_s'(\text{CX}_2)$		2874 m	2954 m		2075 m	2155 m			2969 w
$2\delta_a''(\text{CX}_3)$		2840 w	2848 m		2871 w	2848 w	2069 m	2049 m	2064 m
$\delta_a'(\text{CX}_3)$	1446 s	1441 w	1452 m	1441 s	1443 m	1455 m		1121 w	1119 m
$\gamma'(\text{CX}_2)$	1429 m	1250 w	1419 m		1074 w	1105 s	1423 w	1220 w	1421 s
$\delta_s'(\text{CX}_3)$	1373 w	1363 w	1370 s	1373 w	1365 m	1371 s	1041 s	1087 m	1057 m
								1046 m	1041 s
$\tau''(\text{CX}_2)$	1188 s	1129 m	1199 vs	1059 s	1033 m	1067 vs	1181 s	1190 w	1194 vs
$\nu'(\text{C}-\text{C})$	951 w		949 s	960 m		813 m	905 w		919 m

^a Notation: prime (') = A' symmetry (C_s point group), double prime (") = A'' symmetry (C_s point group); s and a = symmetric and asymmetric (respectively) with respect to the three-fold symmetry axis of the CH_3 group or the two-fold symmetry axis of the CH_2 group. X stands for either H or D. ^b Notation: vs = very strong, s = strong, m = medium, and w = weak. ^c This work. ^d From ref 73.

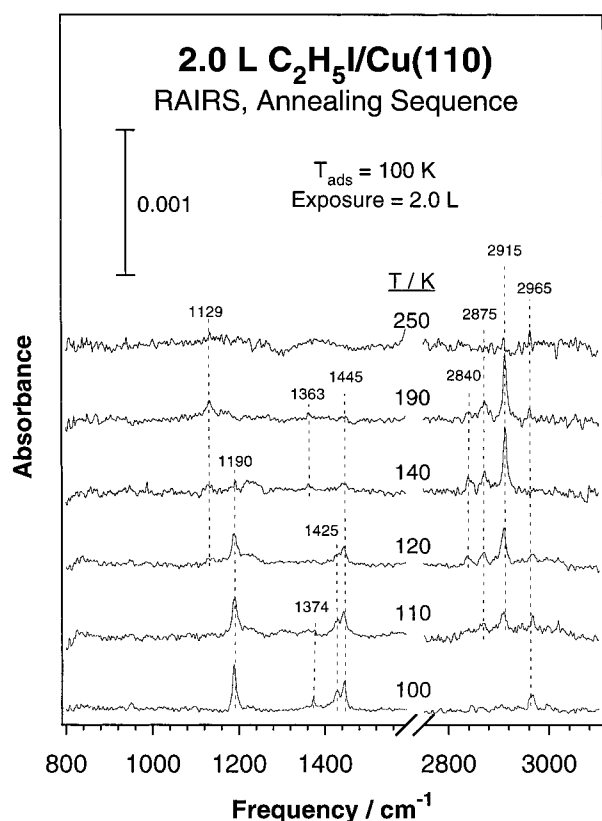


Figure 5. RAIRS annealing sequence for 2.0 L of normal iodoethane on Cu(110) after adsorption at 100 K. The changes seen in the data after heating above 140 K are associated with the scission of the C-I bond and the formation of ethyl surface groups.

surface. Figure 8 shows RAIRS data for methyl, ethyl, 1-propyl, and 2-propyl groups prepared by adsorption of the respective iodoalkanes at 190 K (10.0, 2.0, 3.0, and 2.0 L exposures, respectively). Several clear trends are seen here, especially concerning the signature of terminal methyl moieties, which can be easily identified in all but the methyl case by the peaks associated with the symmetric C-H stretch [$\nu_s'(\text{CH}_3)$] at 2914, 2928, and 2893 cm^{-1} for ethyl, 1-propyl, and 2-propyl, respectively, and with the methyl asymmetric and symmetric deformations [$\delta_a'(\text{CH}_3)$ and $\delta_s'(\text{CH}_3)$] around 1440–1450 and 1360–1370 cm^{-1} , respectively. Notice in particular how the relative intensities of the deformation modes alternate with chain length; the symmetric deformation dominates the spectrum of 1-propyl, but both symmetric and asymmetric modes have low

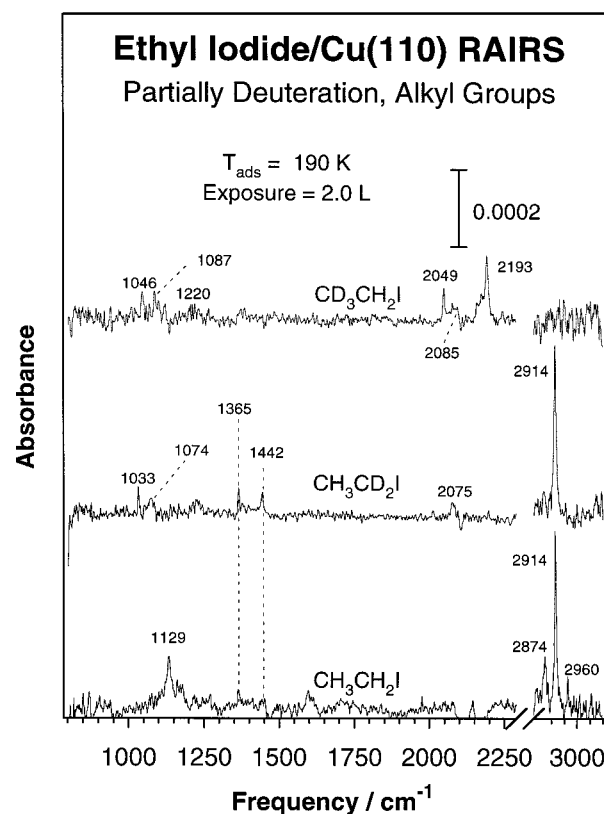


Figure 6. RAIRS data for 2.0 L of $\text{CH}_3\text{CH}_2\text{I}$ (bottom), $\text{CH}_3\text{CD}_2\text{I}$ (middle), and $\text{CD}_3\text{CH}_2\text{I}$ (top) adsorbed on Cu(110) at 190 K. These spectra were used to help in the identification of the methyl and methylene vibrational normal modes of surface ethyl groups.

and comparable signals in the cases of the ethyl and 2-propyl surface species. The methyl surface groups also display a weak peak for the C-H symmetric stretch at 2915 cm^{-1} and a symmetric deformation mode at about 1235 cm^{-1} . Additional signals are seen at 1132 cm^{-1} for the methylene twist in the case of ethyl groups and at 1110 cm^{-1} for the methyl rocking of the propyl surface species.

4. Discussion

On the basis of the infrared data reported here it can be concluded that molecular alkyl iodides adsorbed on Cu(110) display the general behavior seen in other alkyl halide/transition metal systems.^{29,61,62,72,75,76} Specifically, alkyl halides adsorbed

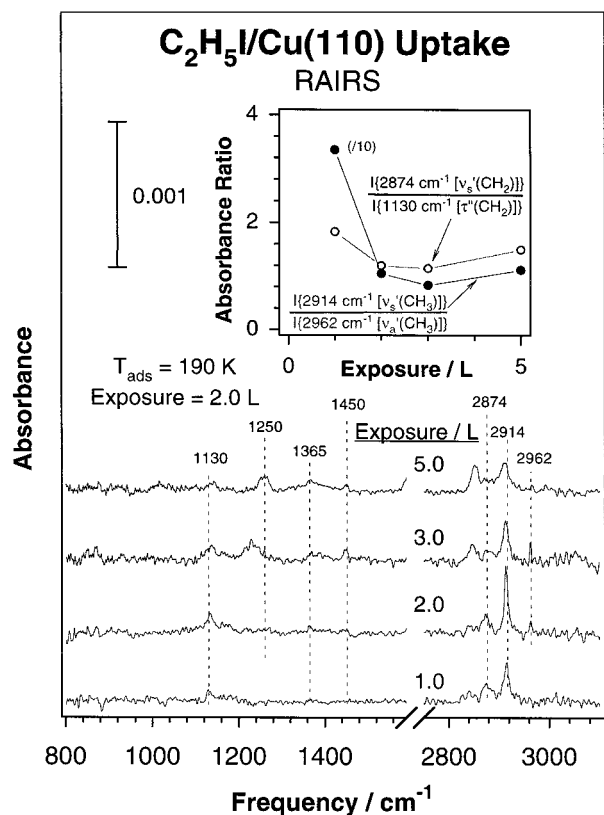


Figure 7. RAIRS data for the uptake of iodoethane on Cu(110) at 190 K. The geometry of the surface alkyl groups changes in a somewhat similar manner as in the case of iodoethane, except that here it is the metal–carbon bond the one that goes from parallel to the surface plane at low coverages to vertical at saturation. Also, because of the absence of a C–I bond, the terminal methyl group flips in the opposite direction (from perpendicular to flat). The inset highlights some of the key intensity changes associated with the change in adsorbate orientation with coverage.

at low temperatures change their adsorption geometries as a function of coverage, from flat to standing up on the surface. Alkyl surface groups, for which much less is known in terms of adsorption geometry, were seen here to display a somewhat similar behavior. The results of these studies are discussed in more detail below.

4.1. Molecularly Adsorbed Alkyl Iodides. Figure 1 provides some information on the adsorption geometry of iodomethane on Cu(110) at 100 K as a function of coverage. In particular, the RAIRS data in that figure display noticeable changes in the relative intensities of the different vibrational peaks as a function of exposure. We start by pointing out that the dynamic dipole moments of the $\delta'_s(\text{CH}_3)$ and $\delta'_a(\text{CH}_3)$ modes are perpendicular to each other, the former lying along the C–I bond and the latter being in the plane perpendicular to it. Thus, based on the surface infrared dipole selection rule mentioned in the Introduction,⁵⁹ it can be established that the weak signal seen for the methyl asymmetric deformation mode [$\delta'_a(\text{CH}_3)$] around 1410 cm^{-1} and the appearance of a strong peak for the methyl symmetric deformation mode [$\delta'_s(\text{CH}_3)$] at 1226 cm^{-1} in the 1.0 L spectrum in Figure 1 arise from an adsorption geometry where the C–I bond is oriented close to perpendicular to the surface. This is corroborated by the presence of the peak assigned to the symmetric C–H stretching mode [$\nu_s(\text{CH}_3)$] around 2910 cm^{-1} in the high-frequency region of the spectrum (the corresponding asymmetric stretching mode appears to be absent, although that could just be because of its low cross section for infrared radiation absorption). The adsorption

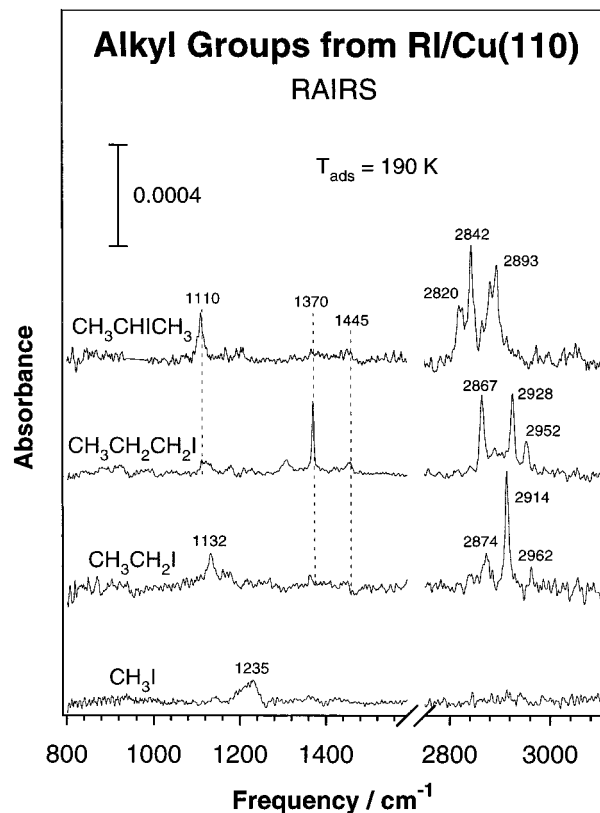


Figure 8. RAIRS data for saturation coverages of methyl (bottom), ethyl (second from bottom), 1-propyl (second from top), and 2-propyl (top) surface groups on Cu(110), prepared by thermal decomposition of the corresponding alkyl iodides (10.0, 2.0, 3.0, and 2.0 L doses, respectively) at 190 K. The adsorption geometries of the metal–carbon are close to vertical to the surface in all cases so that the methyl group axis orientation alternates between standing up and flat on the surface with alkyl chain length.

geometry of the CH_3I at this point cannot be completely standing up, because (1) a small signal is still seen for the methyl asymmetric deformation mode [$\delta'_a(\text{CH}_3)$] around 1410 cm^{-1} and (2) there is also a detectable peak due to the rocking of the methyl group [$\rho(\text{CH}_3)$] about 875 cm^{-1} . In any case, these results are in contrast with those seen on Pt(111), where the molecule was found to lie flatter on the surface at low coverages.^{61,72}

No significant changes are seen in the RAIRS of iodomethane on Cu(110) at low temperatures until reaching doses of 4.0 L or more, at which point a number of subtle changes take place in the vibrational data: (1) the peak around 1410 cm^{-1} corresponding to the $\delta'_a(\text{CH}_3)$ starts to grow, (2) the methyl symmetric deformation [$\delta'_s(\text{CH}_3)$] and C–H stretching [$\nu_s(\text{CH}_3)$] peaks about 1226 and 2910 cm^{-1} , respectively, start to broaden, and (3) the methyl rocking [$\rho(\text{CH}_3)$] mode about 875 cm^{-1} first disappears and then reappears at a slightly higher frequency. Since the features associated with the molecules adsorbed after low doses basically remain unmodified as the coverage is increased, the changes listed above could be interpreted as the result of the population of a second type of iodomethane adsorption state where the molecules are in a more horizontal geometry. This proposal is somewhat similar to that suggested previously for the Au(100) case,⁷⁶ except that in that case the geometries of the first and second CH_3I layers, with their C–I bonds oriented parallel and tilted with respect to the surface, respectively, were opposite to those seen here. Finally, a second set of peaks is seen to develop at 10.0 L because of crystal field splitting in multilayer condensed iodomethane.

A similar analysis can be carried out with the data in Figure 2 for iodoethane molecularly adsorbed on Cu(110). In this case the lack of signal in the spectra for the methyl symmetric deformation mode [$\delta_s'(\text{CH}_3)$] around 1373 cm^{-1} and the presence of a strong methyl asymmetric deformation mode [$\delta_a'(\text{CH}_3)$] at 1444 cm^{-1} after a 1.0 L dose shows that the C–C bond in iodoethane must be oriented close to parallel to the surface at that coverage. Above 2.0 L exposures, on the other hand, the observation of the sharp $\delta_s'(\text{CH}_3)$ (1374 cm^{-1}) peak implies that the molecular axis may be inclined from the surface plane, at least in some of the adsorbates. There is a progressive switch in relative intensities between the symmetric and the asymmetric modes with increasing iodoethane dosing which could be interpreted at first as the result of a gradual change in geometry from flat to standing up. However, the data in Figure 3 strongly argues against this interpretation, since the absolute intensity of the methyl asymmetric deformation peak [$\delta_a'(\text{CH}_3)$] levels off and stays approximately constant after just 1.0 L exposure, while that of the methyl symmetric “umbrella” deformation [$\delta_s'(\text{CH}_3)$] appears only after a 2.0 L dose and grows approximately linearly with exposure afterward. We interpret these observations as being the result of the sequential build-up of two types of iodoethane on the surface, one where the methyl group lies flat on the surface at low coverages and a second with the C–C bond perpendicular to the plane after 1.0 L. This behavior is in sharp contrast to what has been seen on other surfaces, on platinum in particular, where a number of alkyl halides were shown to switch collectively and abruptly from a horizontal to a vertical configuration at the half-saturation point of the uptake,^{61,62} but similar to that of 1-iodopropane on the same Cu(110).²¹

The interpretation above is supported by a few other observations from Figure 2. For one, the methyl symmetric C–H stretching mode [$\nu_s'(\text{CH}_3)$] around 2915 cm^{-1} is only seen for doses above 5.0 L, presumably because it is only then that there are enough molecules with the methyl group standing up on the surface. The methyl asymmetric C–H stretching peak [$\nu_a'(\text{CH}_3)$] about 2960 cm^{-1} , on the other hand, is observed already after 2.0 L, even though its intensity changes do not follow closely those of the methyl asymmetric deformation mode [$\delta_a'(\text{CH}_3)$], as expected. The C–C stretch [$\nu(\text{C–C})$] around 950 cm^{-1} is only visible above 5.0 L, a fact again consistent with a perpendicular geometry growing only at high coverages. Finally, the observation of both scissoring [$\gamma'(\text{CH}_2)$], at 1429 cm^{-1} and twisting [$\tau''(\text{CH}_2)$], at about 1190 cm^{-1}] modes of the methylene group in all spectra imply a tilted geometry for the plane of that moiety.

4.2. Formation of Surface Alkyl Groups. The infrared data presented in Figures 5 and 6 indicate that thermal activation of iodoethane on Cu(110) leads to a chemical transformation which starts about 130 K. As mentioned before, previous work on other systems suggests that the most likely surface intermediate at this stage is ethyl moieties. High-resolution electron energy loss spectroscopy (HREELS) studies on Cu(111) and Cu(110) indicate that the C–I bond in adsorbed iodoalkanes is indeed cleaved by 120 K.³⁰ The same inference was made from photoelectron spectroscopy (XPS) experiments on Pt(111)^{24,72} and Ni(100).^{27,77} Additional RAIRS and static secondary-ion mass spectrometry (SIMS) data support the idea of alkyl formation on metal surfaces at low temperatures in other systems.^{6,8,27,78} Finally, the TPD data for alkyl halides on copper single-crystal surfaces reported in the second accompanying article are in agreement with this interpretation as well.⁶⁶

The RAIRS data obtained here for the iodoethane/Cu(110) case are consistent with the formation of ethyl groups on the surface. For one, it can be seen by the assignment provided in Table 3 that the vibrational modes corresponding to the terminal methyl group in molecular iodoethane are almost unaffected by heating the surface to 190 K. The methylene moieties, on the other hand, are less visible, and do display some changes upon breaking of the C–I bond, as expected by the change in local environment around those fragments. Specifically, in the case of normal (nondeuterated) iodoethane the peaks at 1129, 1250, and 2874 cm^{-1} , assigned here to the $\tau''(\text{CH}_2)$, $\gamma'(\text{CH}_2)$, and $\nu_s'(\text{CH}_2)$ modes of the methylene group in ethyl surface moieties, are red-shifted from their IR values in the solid by between 50 and 170 cm^{-1} upon direct interaction with the copper atoms (see Table 3). Analogous shifts are seen for the corresponding modes of the deuterated methylene groups in the ethyl moieties produced by thermal activation of $\text{CH}_3\text{CD}_2\text{I}$.

Vibrational mode softening similar to that reported above has been observed in a number of high-resolution electron energy loss spectra, in particular for the $\alpha\text{-CH}_2$ group in ethyl and propyl species on Cu(100) and Cu(111),⁷⁹ but was not noted in the RAIRS spectra of ethyl groups on Pt(111).^{62,75} The shifts reported here are presumably the result of charge transfer from the metal into the C–H antibonding orbitals of the CH_2 group,⁷⁹ but the effect of the coadsorbed iodine on the surface cannot be completely ignored. Our assignment is also supported by the similar spectra obtained with organometallic compounds.⁸⁰ Finally, additional RAIRS evidence was obtained for alkyl formation upon thermal activation of alkyl iodides on Cu(110) for the cases of methyl, 1-propyl, and 2-propyl moieties (Figure 8). Notice in particular the blue shifts of both the symmetric deformation [$\delta_s(\text{CH}_3)$] and the symmetric C–H stretching [$\nu_s(\text{CH}_3)$] modes in the surface methyl groups after scission of the C–I bond in iodomethane, again a behavior opposite to that seen in the other alkyl species.

4.3. Adsorption Geometries of Surface Alkyl Groups. In contrast with the case of molecularly adsorbed alkyl halides on metal surfaces, much less is known about the adsorption geometry of the alkyl groups that form upon their thermal activation on the surface. In connection with this, it is noted that both the methyl symmetric and asymmetric deformation modes are present in most of the spectra of surface ethyl groups, at least after exposures in excess of 2.0 L (Figure 7), which means that the axis of such moieties may be somewhat tilted with respect to the surface normal in all cases. Nevertheless, the changes in the spectra as the dose is increased attest to changes in adsorption geometry with coverage. At low coverages, the methyl symmetric C–H stretching mode [$\nu_s'(\text{CH}_3)$] around 2914 cm^{-1} clearly dominates over the weak methyl asymmetric C–H stretching peak [$\nu_a'(\text{CH}_3)$] at 2962 cm^{-1} , suggesting a methyl principal axis close to perpendicular to the surface. After higher doses, however, the asymmetric modes become more visible (until maximizing at 3.0 L), which implies that there is a significant tilting of the methyl groups at saturation. Notice that in this case there is a concomitant decrease in the intensity of the symmetric peak, so the change seen here must involve all the surface species, not just the ones added on. In terms of the CH_2 fragments, their twisting mode [$\tau''(\text{CH}_2)$] around 1130 cm^{-1} is in general more intense than their scissoring vibration [$\gamma'(\text{CH}_2)$] at 1250 cm^{-1} (in particular when compared with the relative intensities of those modes in the solid), an observation that could be explained by the pseudo- C_{2v} axis of the CH_2 group being somewhat flat with respect to the surface. However, the fact that the methylene

Proposed Structures for Alkyl Groups Adsorbed on Cu(110)

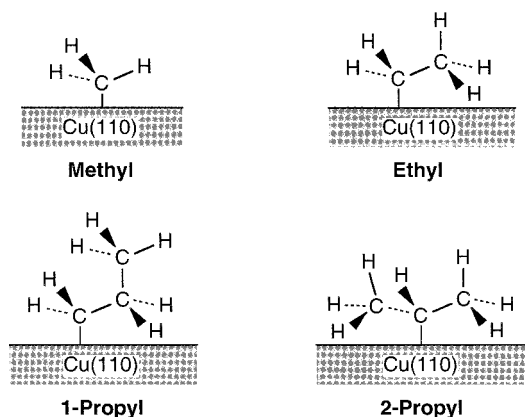


Figure 9. Schematic representation of the structures proposed for the alkyl surface groups on Cu(110) at saturation.

symmetric C–H stretch [$\nu_s'(\text{CH}_2)$] is also visible in this case (around 2874 cm^{-1}) precludes a completely horizontal geometry for those moieties.

It is interesting to compare the RAIRS results from different alkyl groups adsorbed on Cu(110); the data are provided in Figure 8 for saturation coverages of methyl, ethyl, 1-propyl, and 2-propyl species. It can be seen there that the intensities of the methyl symmetric and asymmetric deformation modes are low and approximately equal in the ethyl and 2-propyl cases, allegedly because the terminal methyl groups are significantly tilted with respect to the surface normal (as explained above). In the spectra of the methyl and 1-propyl surface groups, on the other hand, the methyl symmetric deformation clearly dominates, the consequence of the methyl groups standing up on the surface. A similar argument can be made with the data in the C–H stretching region.²¹ Notice, though, that for the adsorbed methyl species there is almost no visible signal in the C–H stretching region at all, presumably because these bands are inherently weak.⁷²

The geometries inferred from the data shown in Figure 8 can be easily understood by assuming that the carbon atoms maintain their tetrahedral bond angles in the alkyl chain upon adsorption. It is assumed that the metal–carbon bond is perpendicular to the surface in all cases, a hypothesis supported by most theoretical calculations^{81–84} as well as by some vibrational experimental results.^{85–87} This immediately places the methyl surface groups from CH_3I decomposition in a standing up geometry, the adsorption geometry proposed here. In the case of the ethyl and 2-propyl moieties, the C–C bonds (and therefore the C_{3v} axis of the terminal methyl groups) would be expected at about $70\text{--}75^\circ$ from the surface normal, again in agreement with our observations. Finally, for 1-propyl groups, two dihedral angles are involved in setting the final geometry of the terminal methyl group, so there is more flexibility on how the moieties may arrange on the surface. We nevertheless propose that at high coverages the most efficient packing would be obtained by adopting an anti configuration around the central C–C bond, an arrangement that would orient the terminal methyl moiety directly perpendicular to the surface (in reality, the methyl groups in the propyl species are slightly tilted, since their asymmetric deformation mode is still visible in their infrared spectrum). The structures proposed here are depicted schematically in Figure 9. Notice that although the molecular alkyl iodides also adsorb in a perpendicular geometry at

saturation, the orientation of the terminal methyl groups in their respective alkyl chains are switch compared to the surface alkyl cases, perhaps because having the metal–iodine bond perpendicular to the surface places the iodine bond to the first carbon at an angle from the surface plane. It should be also noted that even though the RAIRS peak intensities reported here can in general be understood in terms of our proposed bonding geometries, several aspects of the spectra remain unexplained. Specifically, the C–H deformation peaks in the ethyl spectra (Figure 5) are unexpectedly weak in comparison to the C–H stretching modes. Also, some of the symmetry assignments in the C–H stretching region are not entirely consistent with the rest of the spectra. Finally, the presence of other minority species on the surface cannot be ruled out.

It is interesting to extrapolate the conclusions reached in these studies with small alkyl iodides and alkyl groups on Cu(110) surfaces to other more complex systems. As mentioned above, the general trends seen here appear to be quite general to alkyls on metal surfaces.⁶¹ In particular, the alkyl chains appear to align in a vertical geometry upon packing on the metal surface. The same may be true for related adsorbates such as alcohols and alkoxides^{88,89} as well as thiols.^{90,91} A flatter adsorption geometry is often seen at lower coverages, most likely because of the small energy gain due to the van der Waals interaction of the alkyl chains with the surface; this appears to be overcompensated by the gain in adsorption energy of additional molecules with increasing exposures, especially since additional energy is released by the weak alkyl–alkyl attractions. As the alkyl chains grow in size, the standing up configuration must become more favorable, because the long chains in molecules such as thiols self-assemble easily on metal surfaces.^{92,93} The resulting monolayer films are usually densely packed, well-ordered with alkyl chains in an all-trans conformation at an average tilt angle between 28° and 40° from the surface normal. The propyl molecular axis in our proposed structure comes out to be approximately 35° from the surface normal, a value within the range of that seen in the self-assembled monolayers.

5. Conclusions

The bonding geometry of iodomethane, iodoethane, 1-iodopropane, and 2-iodopropane adsorbed molecularly on Cu(110) was determined by reflection–absorption infrared spectroscopy. The methyl moieties in iodomethane were seen to adsorb in a close to perpendicular geometry at low coverages but to tilt somewhat at saturation, a behavior opposite to that seen for alkyl halides on Pt(111). Iodoethane roughly follows the behavior observed in other systems, namely, it adsorbs in a flat-lying configuration at low coverages and stands up at higher coverages. However, in contrast to the Pt(111) case, there is no collective rearrangement of the alkyl chains upon increasing coverage, only the new adsorbates adopt the vertical adsorption configuration.

Annealing of all the adsorbed alkyl iodides studied here at temperatures above 140 K results in the dissociation of the C–I bond and in the formation of the corresponding alkyl groups. Identification of those moieties was aided in the case of iodoethane by additional studies with partially deuterated compounds. The surface alkyl groups were found to change their adsorption geometry with changing coverage as well, in this case by adopting a slightly different vertical structure at saturation. As a result of this, an interesting alternation in the orientation of the terminal methyl groups was observed with increasing hydrocarbon chain size. The behavior reported here appears to be quite general to alkyl-containing species adsorbed

on metal surfaces, and is also consistent with the growth of self-assembled monolayers.

Acknowledgment. Financial support for this project was provided by the National Science Foundation under Grant CHE-9819652.

References and Notes

- (1) Hurd, D. T.; Rochow, E. G. *J. Am. Chem. Soc.* **1945**, *67*, 1057.
- (2) Petrov, A. D.; Mironov, B. F.; Ponomarenko, V. A.; Chernyshev, E. A. *Synthesis of Organosilicon Monomers*; Consultants Bureau: New York, 1964.
- (3) Sun, D. H.; Bent, B. E.; Wright, A. P.; Naasz, B. M. *J. Mol. Catal. A* **1998**, *131*, 169.
- (4) Fanta, P. E. *Synthesis* **1974**, 9.
- (5) Xi, M.; Bent, B. E. *J. Am. Chem. Soc.* **1993**, *115*, 7426.
- (6) Zaera, F. *Acc. Chem. Res.* **1992**, *25*, 260.
- (7) Zaera, F. *Chem. Rev.* **1995**, *95*, 2651.
- (8) Zaera, F. *J. Mol. Catal.* **1994**, *86*, 221.
- (9) Bent, B. E. *Chem. Rev.* **1996**, *96*, 1361.
- (10) Chiang, C. M.; Wentzlaff, T. H.; Jenks, C. J.; Bent, B. E. *J. Vac. Sci. Technol. A* **1992**, *10*, 2185.
- (11) Chiang, C.-M.; Wentzlaff, T. H.; Bent, B. E. *J. Phys. Chem.* **1992**, *96*, 1836.
- (12) Chiang, C.-M.; Bent, B. E. *Surf. Sci.* **1992**, *279*, 79.
- (13) Lin, J.-L.; Bent, B. E. *J. Am. Chem. Soc.* **1993**, *115*, 6943.
- (14) Lin, J. L.; Chiang, C. M.; Jenks, C. J.; Yang, M. X.; Wentzlaff, T. H.; Bent, B. E. *J. Catal.* **1994**, *147*, 250.
- (15) Xi, M.; Bent, B. E. *Surf. Sci.* **1992**, *278*, 19.
- (16) Xi, M.; Bent, B. E. *Langmuir* **1994**, *10*, 505.
- (17) Paul, A. M.; Bent, B. E. *J. Catal.* **1994**, *147*, 264.
- (18) Kash, P. W.; Sun, D. H.; Xi, M.; Flynn, G. W.; Bent, B. E. *J. Phys. Chem.* **1996**, *100*, 16621.
- (19) Jenks, C. J.; Chiang, C.-M.; Bent, B. E. *J. Am. Chem. Soc.* **1991**, *113*, 6308.
- (20) Jenks, C. J. Ph.D. Thesis, Columbia University, 1992.
- (21) Jenks, C. J.; Bent, B. E.; Bernstein, N.; Zaera, F. *J. Am. Chem. Soc.* **1993**, *115*, 308.
- (22) Jenks, C. J.; Xi, M.; Yang, M. X.; Bent, B. E. *J. Phys. Chem.* **1994**, *98*, 2152.
- (23) Forbes, J. G.; Gellman, A. J. *J. Am. Chem. Soc.* **1993**, *115*, 6277.
- (24) Zaera, F. *Surf. Sci.* **1989**, *219*, 453.
- (25) Zaera, F. *J. Am. Chem. Soc.* **1989**, *111*, 8744.
- (26) Zaera, F. *J. Phys. Chem.* **1990**, *94*, 8350.
- (27) Tjandra, S.; Zaera, F. *Surf. Sci.* **1993**, *289*, 255.
- (28) Tjandra, S.; Zaera, F. *Langmuir* **1994**, *10*, 2640.
- (29) Tjandra, S.; Zaera, F. *J. Am. Chem. Soc.* **1995**, *117*, 9749.
- (30) Lin, J.-L.; Bent, B. E. *J. Phys. Chem.* **1992**, *96*, 8529.
- (31) Lin, J.-L.; Teplyakov, A. V.; Bent, B. E. *J. Phys. Chem.* **1996**, *100*, 10721.
- (32) Yang, M. X.; Sarkar, S.; Bent, B. E.; Bare, S. R.; Holbrook, M. T. *Langmuir* **1997**, *13*, 229.
- (33) Dautzenberg, F. M.; Platteeuw, J. C. *J. Catal.* **1972**, *24*, 364.
- (34) Anderson, J. R.; Shimoyama, Y. In *Proceedings of the 5th International Congress on Catalysis*; Miami Beach, Florida, August 20–26, 1972; Hightower, J. W., Ed.; North-Holland Publishing Co.: Amsterdam, 1973; p 695.
- (35) Dartigues, J.-M.; Chambellan, A.; Gault, F. G. *J. Am. Chem. Soc.* **1976**, *98*, 856.
- (36) Davis, S. M.; Zaera, F.; Somorjai, G. A. *J. Catal.* **1984**, *85*, 206.
- (37) Zaera, F. *Isr. J. Chem.* **1998**, *38*, 293.
- (38) Zaera, F.; Kollin, E.; Gland, J. L. *Chem. Phys. Lett.* **1985**, *121*, 464.
- (39) Moon, D. W.; Cameron, S.; Zaera, F.; Eberhardt, W.; Carr, R.; Bernasek, S. L.; Gland, J. L.; Dwyer, D. J. *Surf. Sci.* **1987**, *180*, L123.
- (40) Fulmer, J. P.; Zaera, F.; Tysoe, W. T. *J. Chem. Phys.* **1987**, *87*, 7265.
- (41) Wang, S. W.; Ogletree, D. F.; Van Hove, M. A.; Somorjai, G. A. *Adv. Quantum Chem.* **1989**, *20*, 2.
- (42) Pendry, J. B. *Surf. Sci. Rep.* **1993**, *19*, 87.
- (43) Starke, U.; Pendry, J. B.; Heinz, K. *Prog. Surf. Sci.* **1996**, *52*, 53.
- (44) Van Hove, M. A.; Somorjai, G. A. *J. Mol. Catal. A* **1998**, *131*, 243.
- (45) Fadley, C. S.; Van Hove, M. A.; Hussain, Z.; Kaduwela, A. P.; Couch, R. E.; Kim, Y. J.; Len, P. M.; Palomares, J.; Ryce, S.; Ruebush, S.; Tober, E. D.; Wang, Z.; Ynzunka, R. X.; Daimon, H.; Galloway, H.; Salmeron, M. B.; Schattke, W. *Surf. Rev. Lett.* **1997**, *4*, 421.
- (46) Bradshaw, A. M. *Curr. Opin. Solid State Mater. Sci.* **1997**, *2*, 530.
- (47) Wang, L. P.; Tysoe, W. T.; Ormerod, R. M.; Lambert, R. M.; Hoffmann, H.; Zaera, F. *J. Phys. Chem.* **1990**, *94*, 4236.
- (48) Hoffmann, H.; Zaera, F.; Ormerod, R. M.; Lambert, R. M.; Wang, L. P.; Tysoe, W. T. *Surf. Sci.* **1990**, *232*, 259.
- (49) Netzer, F. P.; Ramsey, M. G. *Crit. Rev. Solid State Mater. Sci.* **1992**, *17*, 397.
- (50) Zaera, F.; Fischer, D. A.; Carr, R. G.; Gland, J. L. *J. Chem. Phys.* **1988**, *89*, 5335.
- (51) Zaera, F. *X-ray Absorption Fine Structure for Catalysis and Surfaces*; Iwasawa, Y., Ed.; World Scientific: Singapore, 1996; p 362.
- (52) Stöhr, J. *NEXAFS Spectroscopy*; Springer-Verlag: Berlin, 1992.
- (53) Bradshaw, A. M. *Appl. Surf. Sci.* **1982**, *11/12*, 712.
- (54) Hoffmann, F. M. *Surf. Sci. Rep.* **1983**, *3*, 107.
- (55) Chabal, Y. J. *Surf. Sci. Rep.* **1988**, *8*, 211.
- (56) Zaera, F. In *Encyclopedia of Chemical Physics and Physical Chemistry*; Moore, J. H., Spencer, N. D., Eds.; IOP Publishing Inc.: Philadelphia, in press.
- (57) Nakamoto, K. *Infrared and Raman Spectra of Inorganic and Coordination Compounds*, 3rd ed.; Wiley-Interscience: New York, 1978.
- (58) Socrates, G. *Infrared Characteristic Group Frequencies: Tables and Charts*, 2nd ed.; Wiley: Chichester, 1994.
- (59) Greenler, R. G. *J. Chem. Phys.* **1966**, *44*, 310.
- (60) Parikh, A. N.; Allara, D. L. *J. Chem. Phys.* **1992**, *96*, 927.
- (61) Zaera, F.; Hoffmann, H.; Griffiths, P. R. *J. Electron Spectrosc. Relat. Phenom.* **1990**, *54/55*, 705.
- (62) Hoffmann, H.; Griffiths, P. R.; Zaera, F. *Surf. Sci.* **1992**, *262*, 141.
- (63) Jenks, C. J.; Bent, B. E.; Bernstein, N.; Zaera, F. *Surf. Sci.* **1992**, *277*, L89.
- (64) Janssens, T. V. W.; Zaera, F. *J. Phys. Chem.* **1996**, *100*, 14118.
- (65) Street, S. C.; Gellman, A. J. *J. Chem. Phys.* **1996**, *105*, 7158.
- (66) Jenks, C. J.; Bent, B. E.; Zaera, F. *J. Phys. Chem. B* **2000**, *104*, 3017.
- (67) de Jesús, J. C.; Zaera, F. *Surf. Sci.* **1999**, *430*, 99.
- (68) Herzberg, G. *Molecular Spectra and Molecular Structure. II. Infrared and Raman Spectra of Polyatomic Molecules*; Van Nostrand Reinhold: New York, 1945.
- (69) Sverdlov, L. M.; Kovner, M. A.; Krainov, E. P. *Vibrational Spectra of Polyatomic Molecules*; John Wiley & Sons: New York, 1974.
- (70) *The Aldrich Library of Infrared Spectra*, 1st ed.; Aldrich Chemical Co.: Milwaukee, WI.
- (71) Dows, D. A. *J. Chem. Phys.* **1958**, *29*, 484.
- (72) Zaera, F.; Hoffmann, H. *J. Phys. Chem.* **1991**, *95*, 6297.
- (73) Durig, J. R.; Thompson, J. W.; Thyagesan, V. W.; Witt, J. D. *J. Mol. Struct.* **1975**, *24*, 41.
- (74) Crowder, G. A. *J. Mol. Spectrosc.* **1973**, *48*, 467.
- (75) Zaera, F.; Hoffmann, H.; Griffiths, P. R. *Vacuum* **1990**, *41*, 735.
- (76) Yang, M. X.; Jo, S. K.; Paul, A.; Avila, L.; Bent, B. E.; Nishikida, K. *Surf. Sci.* **1995**, *325*, 102.
- (77) Tjandra, S.; Zaera, F. *J. Vac. Sci. Technol.* **1992**, *A10*, 404.
- (78) Tjandra, S.; Zaera, F. *Langmuir* **1992**, *8*, 2090.
- (79) Lin, J.-L.; Bent, B. E. *Chem. Phys. Lett.* **1992**, *194*, 208.
- (80) Maslowsky, E., Jr. *Vibrational Spectra of Organometallic Compounds*; John Wiley & Sons: New York, 1977.
- (81) Yang, H.; Whitten, J. L. *J. Am. Chem. Soc.* **1991**, *113*, 6442.
- (82) Siegbahn, P. E. M.; Panas, I. *Surf. Sci.* **1990**, *240*, 37.
- (83) Burghgraef, H.; Jansen, A. P. J.; van Santen, R. A. *Surf. Sci.* **1995**, *324*, 345.
- (84) Kua, J.; Goddard, W. A. *J. Phys. Chem. B* **1998**, *102*, 9492.
- (85) Fairbrother, D. H.; Peng, X. D.; Viswanathan, R.; Stair, P. C.; Trenary, M.; Fan, J. *Surf. Sci.* **1993**, *285*, L455.
- (86) French, C.; Harrison, I. *Surf. Sci.* **1995**, *342*, 85.
- (87) Yang, Q. Y.; Maynard, K. J.; Johnson, A. D.; Ceyer, S. T. *J. Chem. Phys.* **1995**, *102*, 7734.
- (88) Street, S. C.; Gellman, A. J. *J. Phys. Chem.* **1996**, *100*, 8338.
- (89) Street, S. C.; Gellman, A. J. *Surf. Sci.* **1997**, *372*, 223.
- (90) Fernandez, A.; Espinos, J. P.; Gonzalez Elipse, A. R.; Kerker, M.; Thompson, P. B. J.; Ludecke, J.; Scragg, G.; Decarvalho, A. V.; Woodruff, D. P.; Fernandez Garcia, M.; Conesa, J. C. *J. Phys. Condens. Matter* **1995**, *7*, 7781.
- (91) Napier, M. E.; Friend, C. M. *Langmuir* **1996**, *12*, 1800.
- (92) Nuzzo, R. G.; Dubois, L. H.; Allara, D. L. *J. Am. Chem. Soc.* **1990**, *112*, 558.
- (93) Hoffmann, H.; Mayer, U.; Brunner, H.; Krischanitz, A. *Vib. Spectrosc.* **1995**, *8*, 151.